PERGAMON

Engineering Fracture Mechanics 63 (1999) 631–648

Engineering Fracture Mechanics

www.elsevier.com/locate/engfracmech

A fast iterative boundary element method for solving closed crack problems

Niell Elvin*, Christopher Leung

Department of Civil and Environmental Engineering, Massachusetts Institute of Technology, PO Box 397123, Cambridge MA 02139, USA

Received 25 June 1998; accepted 9 December 1998

Abstract

This paper describes an iterative hybrid boundary element method for solving non-linear closed crack problems. The original crack problem is split into two separate sub-problems: (1) the exterior body (without crack) which is modeled using displacement discontinuity boundary elements, and (2) the crack in an infinite domain which is modeled using either a dislocation density or displacement discontinuity approach. Iteration is performed between the exterior body and the crack faces until all boundary conditions are satisfied. Several advantages of this method over previous methods are discussed and are demonstrated in example problems.

Keywords: Boundary element method; Closed cracks; Iterative technique

1. Introduction

The understanding of crack closure is important in predicting the static and fatigue strength of structures subjected to compressive stresses. This problem has been extensively studied by many authors using various numerical, experimental and analytical techniques [1]. The two most frequently used numerical techniques for studying fracture mechanics problems are the finite element method (FEM) and boundary element method (BEM). The main advantage of the BEM over FEM is that only the domain boundaries need to be discretized. Contact can be

* Corresponding author. Tel.: +1-617-323-7700 ext. 6291; fax: +1-617-363-5709.
E-mail address: atlaselv@mit.edu (N. Elvin)

0013-7944/99/$ - see front matter
PII: S0013-7944(99)00035-1

easily included in the BEM since all the unknowns of the problem, such as the contact tractions and displacements, are boundary quantities. The BEM has another advantage of being, particularly, adept in calculating important fracture mechanics parameters such as stress intensity factors (SIF) and crack growth directions. One drawback of the BEM is that in most BEMs the associated matrices are nonsymmetric and are fully populated. It must be noted that symmetric coefficient matrices can be achieved using a Galerkin symmetric BEM. However, these methods at present only offer slightly improved solution over the traditional solution methods (see, for example, [2]).

Various BEMs have been proposed for solving crack problems. One frequently used BEM is the subregion method, described in Ref. [3]. In the subregion method, the cracked body is subdivided into two subregions and the traction and displacements along all common nodes not on the crack faces are constrained to have equal displacements. The problem with the subregion method is that the resulting matrices tend to be large due to the extra nodes along the subregion interfaces which do not lie along the boundary of the body. Crouch [4] has developed the displacement discontinuity boundary element method (DDBEM), which overcomes the problem associated with the constrained nodes in the subregion method.

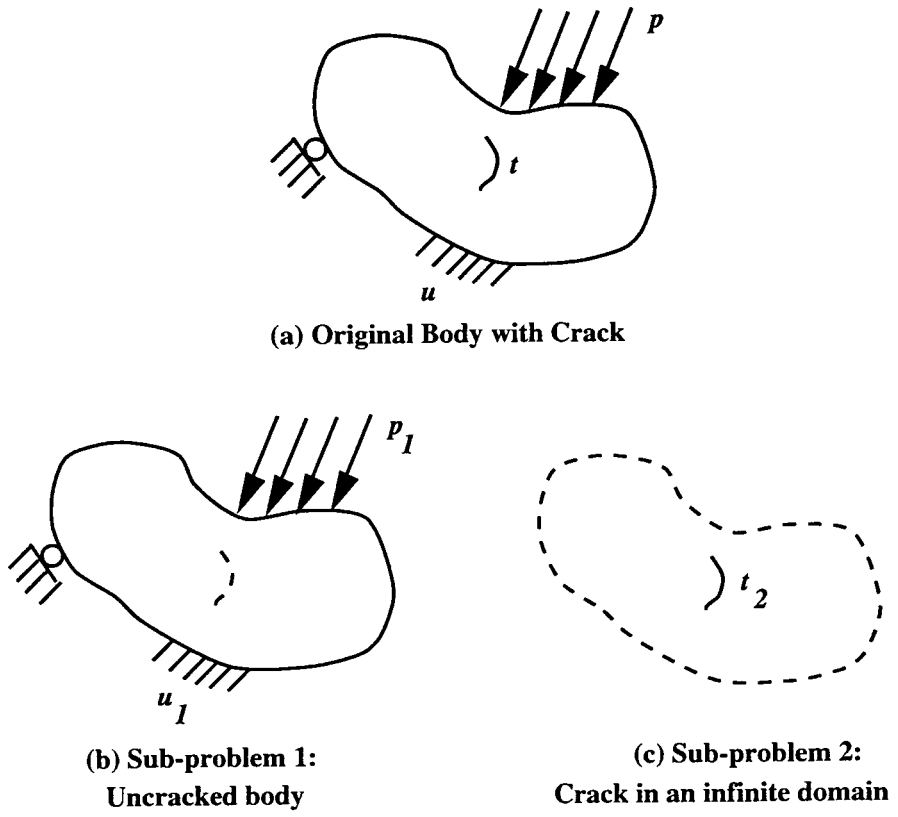

Fig. 1. Schematic representation of the iterative method of solving crack problems after Ameen and Raghuprasad [8].

Another frequently used BEM, which obviates the need for multidomains, is the 'dual boundary element' approaches [5–7]. In this method, the displacement boundary integral equation is applied to one of the crack faces and the traction boundary integral equation on the other.

Other methods have also been used to solve the open crack problem, but have not yet been extended to the closed crack problem. An iterative method was proposed by Ameen and Raghuprasad [8]. In this method, the body is subdivided into two sub-problems as shown in Fig. 1. Sub-problem 1 models the body subjected to the prescribed force and displacement boundary conditions without the crack. Sub-problem 2 models a crack in an infinite domain subjected to internal shear and normal tractions. Iteration between the two sub-problems is then performed until all the boundary conditions in both bodies are satisfied. The final solution for the unknowns is a superposition of the unknowns of the two bodies. Ameen and Raghuprasad [8] did not consider closed cracks and commented that the only advantage of their iterative method over other methods, such as the DDBEM, is that the matrix associated with each region requires less storage space than the combined problem and, thus, can be handled by computers with smaller memory storage.

Another method discussed by Sturt [9] uses a hybrid method in which the DDBEM is used to model the outer boundaries of the structure, while a distributed dislocation technique (DDT) is used to model the crack. The greatest advantage of the DDT is that the stress tip singularities are accurately calculated. Sturt [9] did not consider crack closure, though the DDT can be extended to include this case. Xu and Ortiz [10] have developed an energy based dislocation density approach, which leads to symmetric coefficient matrices and integral equations which are only mildly singular and can, thus, be integrated with a simple quadrature scheme.

This paper discusses a coupled iterative-hybrid boundary element method (IHBEM). In this method, the two bodies are modeled separately as described by Ameen and Raghuprasad [8]. Sub-problem 2 is modeled either by using the DDT or DDBEM. The advantage of the IHBEM is that since contact problems are non-linear, iteration is typically required for all solution methods, and since the IHBEM iterates on smaller matrices, the method can potentially prove to be faster than traditional techniques. The method has the added advantage that any standard BEM code can be easily modified to obtain results for the crack-free region.

Closed crack simulation is particularly important in the study of subsurface crack growth under rolling contact and, thus, this problem has been extensively studied by various authors [14–16]. A subsurface crack under rolling contact has been chosen as one of the example problems to illustrate the IHBEM, since it reveals some further subtle advantages of this method.

2. Theoretical formulation

A two-dimensional cracked body shown in Fig. 1(a) is subjected to prescribed tractions (p) and displacements (u) on the outer boundary, and tractions (t) on the crack surface. The body is assumed to be linearly elastic, homogenous and isotropic. The problem is first partitioned into two subregions. Sub-problem 1, shown in Fig. 1(b), represents the original body without

the crack subjected to all the external boundary conditions (p_1 and u_1). Sub-problem 2, shown in Fig. 1(c), represents a crack in an infinite body subjected to prescribed tractions (t_2). Any BEM can be used to solve the boundary value problem for both sub-problems. In this paper, however, sub-problem 1 is solved using the quadratic displacement discontinuity (QDD) method [11]. Sub-problem 2 is solved using either the DDT or QDD method. After sub-problem 1 is solved, the normal and shear tractions are calculated at the position of crack (t_2). These tractions are then applied as negative forces on the crack-faces of sub-problem 2. Sub-problem 2 is then solved, and the boundary conditions on the boundaries of sub-problem 1 are calculated. These boundary conditions are then subtracted from the existing boundary conditions (p) of sub-problem 1 and the tractions at the crack are recalculated. The iterations between sub-problems 1 and 2 are performed until convergence is achieved.

2.1. Background to the QDD method

In the DDT, the analyzed body is subdivided into a series of N elements with unknown displacement discontinuities over each one. The unknown displacement discontinuities are then solved by summing the effects of all N elements so as to satisfy the prescribed boundary conditions. If stresses are prescribed on the ith element then the ith equations of the system are

$$
\begin{aligned}
{}^{i}\sigma_{\mathrm{s}} &= \sum_{j=1}^{N} {}^{ij}A_{\mathrm{ss}}{}^{j}D_{\mathrm{s}} + \sum_{j=1}^{N} {}^{ij}A_{\mathrm{sn}}{}^{j}D_{\mathrm{n}} \\
{}^{i}\sigma_{\mathrm{n}} &= \sum_{j=1}^{N} {}^{ij}A_{\mathrm{ns}}{}^{j}D_{\mathrm{s}} + \sum_{j=1}^{N} {}^{ij}A_{\mathrm{nn}}{}^{j}D_{\mathrm{n}}
\end{aligned}
\tag{1}
$$

Similarly for the prescribed displacements

$$
{}^{i}u_{\mathrm{s}} = \sum_{j=1}^{N} {}^{ij}B_{\mathrm{ss}}{}^{j}D_{\mathrm{s}} + \sum_{j=1}^{N} {}^{ij}B_{\mathrm{sn}}{}^{j}D_{\mathrm{n}}
$$

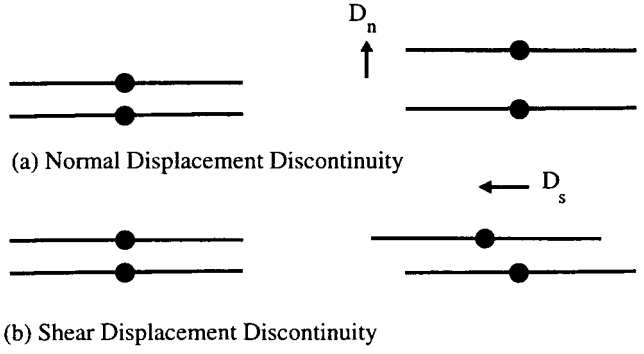

Fig. 2. Schematic representation of normal and shear displacement discontinuities.

$$^{i}u_{\mathrm{n}} = \sum_{j=1}^{N} {}^{ij}B_{\mathrm{ns}}{}^{j}D_{\mathrm{s}} + \sum_{j=1}^{N} {}^{ij}B_{\mathrm{nn}}{}^{j}D_{\mathrm{n}} \tag{2}$$

where σ_{s} and σ_{n} are the tangential and normal stresses, respectively. ${}^{ij}A$ and ${}^{ij}B$ are the stress and displacement influence coefficients, respectively, which relate the stresses (or displacements) of node i to a unit displacement discontinuity at node j. D_{s} and D_{n} are the shear and normal displacement discontinuities, respectively, which represent the relative displacements between the faces of a crack as shown in Fig. 2. In the case of an assumed quadratic variation in displacement discontinuity, Bhattacharyya and Willment [11] have shown that

$$\boldsymbol{D} = \boldsymbol{D}(-b)\left[\frac{1}{2b^2}x(x-b)\right] + \boldsymbol{D}(0)\left[1-\frac{x^2}{b^2}\right] + \boldsymbol{D}(b)\left[\frac{1}{2b^2}x(x+b)\right] \tag{3}$$

where $\boldsymbol{D}$ has components D_{s} and D_{n}, and needs to be evaluated at three points (nodes) along the element. In general, the nodes can be placed at any position within the element except the element end-points, where numerical problems occur due to the interpolation function (in Eq. (3)) not being differentiable across elements. In Eq. (3), the nodes are placed at $x = -b$, $x = 0$ and $x = b$. The influence coefficients ${}^{ij}A$ and ${}^{ij}B$ for the QDD have analytical representations and are given by Bhattacharyya and Willment [11]. Eqs. (1) and (2) can be formulated in matrix form as

$$\{\boldsymbol{b}\} = [\boldsymbol{C}]\{\boldsymbol{D}\} \tag{4}$$

where vector $\{\boldsymbol{b}\}$ are the prescribed boundary conditions, $[\boldsymbol{C}]$ is the influence function matrix and $\{\boldsymbol{D}\}$ is the displacement discontinuity vector. Once $\{\boldsymbol{D}\}$ is calculated, the stresses and displacements $\{\boldsymbol{f}_1\}$ for any set of interior points can be calculated using

$$\{\boldsymbol{f}_1\} = [\boldsymbol{E}_1]\{\boldsymbol{D}\} \tag{5}$$

where $[\boldsymbol{E}_1]$ is the influence matrix relating the stresses and displacements of the interior point to the boundary displacement discontinuities.

2.2. Background to the DDT method

Consider a single dislocation of Burger's vector $\boldsymbol{b}$ (with components b_x and b_y) located at

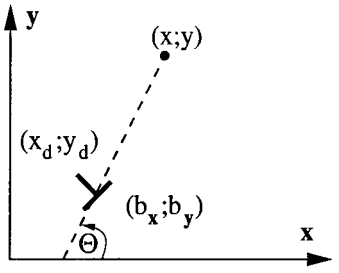

Fig. 3. A dislocation with Burger's vector (b_x and b_y) in an infinite elastic space.

(x_d,y_d) in an infinite elastic domain, shown in Fig. 3. The resulting stresses and displacements at a second point (x,y) are [12]

$$\sigma_{xx}(x,y) = 2\frac{\mu}{\pi(\kappa+1)}\{b_x G_{xxx} + b_y G_{yxx}\} \tag{6}$$

$$\sigma_{yy}(x,y) = 2\frac{\mu}{\pi(\kappa+1)}\{b_x G_{xyy} + b_y G_{yyy}\} \tag{7}$$

$$\sigma_{xy}(x,y) = 2\frac{\mu}{\pi(\kappa+1)}\{b_x G_{xxy} + b_y G_{yxy}\} \tag{8}$$

$$u_x(x,y) = \frac{1}{2\pi(\kappa+1)}\{b_x U_{xx} + b_y U_{yx}\} \tag{9}$$

$$u_y(x,y) = \frac{1}{2\pi(\kappa+1)}\{b_x U_{xy} + b_y U_{yy}\} \tag{10}$$

where μ is the shear modulus, $\kappa = 3 - 4\nu$ in plane strain (ν being the Poisson's ratio). G_{lmn} and U_{ij} are the stress and displacement dislocation influence coefficients, respectively, given in Appendix A.

Consider a crack of length $2a$ with local co-ordinates x and y shown in Fig. 4. By placing a dislocation density $\boldsymbol{B}$ (with components B_x and B_y) over the crack, the stresses and displacements at any point (x,y) can be calculated using

$$\sigma_{ij}(x,y) = 2\frac{\mu}{\pi(\kappa+1)}\int_{-a}^{a}\left(B_x U_{\hat{x}ij}(x,y,\xi,0) + B_y G_{\hat{y}ij}(x,y,\xi,0)\right)\mathrm{d}\xi \tag{11}$$

$$u_i(x,y) = \frac{1}{2\pi(\kappa+1)}\int_{-a}^{a}\left(B_x U_{i\hat{x}}(x,y,\xi,0) + B_y U_{i\hat{y}}(x,y,\xi,0)\right)\mathrm{d}\xi \tag{12}$$

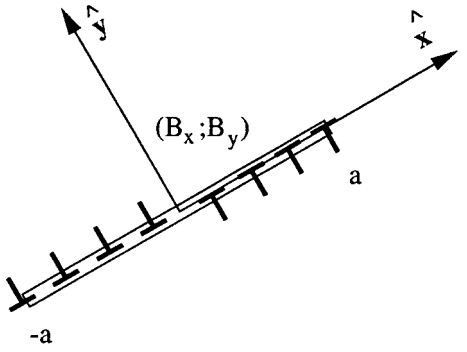

Fig. 4. A crack modeled by a distribution of dislocation densities (B_x and B_y).

where $B_k = \mathrm{d}b_k/\mathrm{d}\hat{x}$, $G_{\hat{k}ij}$ and $U_{i\hat{k}}$ are the local coordinate stress and displacement influence functions for a Burger's vector density in the k direction, respectively. A standard tensor coordinate transformation is needed to map the global influence functions to the local coordinates (see Ref. [12]). It must be noted that in general the integrals in Eqs. (11) and (12) contain singularities of the order $1/\sqrt{d}$, which cannot be solved analytically and require special numerical integration techniques, such as Gauss–Chebyshev quadrature. (For full explanation of Gauss–Chebyshev quadrature, see Ref. [12]). Since there is a $-1/2$ singularity at the crack tip, B_k can be expressed as $B_k = \phi_k/\sqrt{a^2 - x^2}$, where ϕ_k is a non-singular function. After numerical integration, Eqs. (11) and (12) can be rewritten as

$$\{T\} = [G]\{\Phi\} \tag{13}$$

where vector $\{\boldsymbol{T}\}$ corresponds to the prescribed boundary conditions, $[\boldsymbol{G}]$ is the dislocation influence matrix and vector $\{\Phi\}$ represents the unknowns ϕ_k. Once $\{\Phi\}$ is computed, the unknown dislocation density $\boldsymbol{B}$ can be obtained. Eqs. (11) and (12) can also be used to calculate the stresses and displacements $\{\boldsymbol{f}_2\}$ at any point in the domain using

$$\{\boldsymbol{f}_2\} = [\boldsymbol{E}_2]\{\boldsymbol{B}\} \tag{14}$$

where $[\boldsymbol{E}_2]$ is the influence matrix relating the stresses and displacements of the interior point to the dislocation densities.

2.3. Background to the analysis of closed crack

Consider a partially closed crack of length $2a$, shown in Fig. 5. For each pair of corresponding particles located on either face of the closed portion of the crack, the relative normal displacement are constrained to be equal and the shear tractions are related to the normal tractions through a friction law. In the case of Coulomb friction, the crack faces will stick and the relative shear displacement will be zero if

$$|S| < c + fN \tag{15}$$

where S and N are the shear and normal tractions along the closed portion of the crack, and c and f are the cohesion and the coefficient of friction, respectively. In the case when the shear

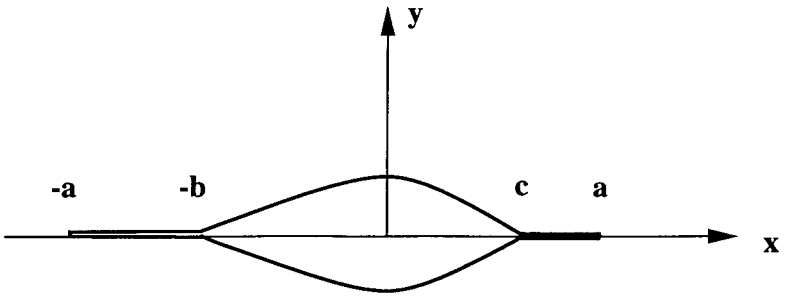

Fig. 5. A schematic depiction of a partially closed crack.

traction (S) is sufficiently large to overcome stick, the shearing traction is limited by friction, i.e.,

$$|S| = c + fN \tag{16}$$

For the crack shown in Fig. 5, the location of the crack-closure points b and c, as well as the stick/slip conditions are unknown and need to be found as part of the solution. Although the DDT can be used to solve crack-closure problems, the resulting integral equations tend to require complicated formulation which are beyond the scope of this paper and the interested reader is referred to [12].

A more practical method for solving closed crack problems is given by Crouch [13], in which the crack surfaces are connected by springs with constant normal stiffness K_n and shear stiffness K_s so that

$$^{i}S = K_s{}^{i}D_s$$

$$^{i}N = K_n{}^{i}D_n \tag{17}$$

Now, combining Eqs. (1) and (17) gives

$$0 = -K_s{}^{i}D_s + \sum_{j=1}^{N} {}^{ij}A_{ss}{}^{j}D_s + \sum_{j=1}^{N} {}^{ij}A_{sn}{}^{j}D_n$$

$$0 = -K_n{}^{i}D_n + \sum_{j=1}^{N} {}^{ij}A_{ns}{}^{j}D_s + \sum_{j=1}^{N} {}^{ij}A_{nn}{}^{j}D_n \tag{18}$$

By choosing relatively large values of K_n and K_s, the faces of the crack can be prevented from relative deformations. In general, crack-closure problems are path dependent which means that load incrementation is needed to find the final displacement and stress state of the body. At any load step (k), the shear and normal tractions calculated in Eq. (17) have to be compared with the Coulomb friction criterion given by Eq. (15). If the shear traction S is sufficiently large to overcome stick, Eqs. (16) and (1) need to be used giving

$$c + fN = \sum_{j=1}^{N} {}^{ij}A_{ss}{}^{j}D_s + \sum_{j=1}^{N} {}^{ij}A_{sn}{}^{j}D_n$$

$$0 = -K_n{}^{i}D_n + \sum_{j=1}^{N} {}^{ij}A_{ns}{}^{j}D_s + \sum_{j=1}^{N} {}^{ij}A_{nn}{}^{j}D_n \tag{19}$$

At any load increment, the normal tractions on the faces can be negative indicating separation of the crack faces. In this case, the crack faces are stress free and Eq. (1) becomes

$$0 = \sum_{j=1}^{N} {}^{ij}A_{ss}{}^{j}D_s + \sum_{j=1}^{N} {}^{ij}A_{sn}{}^{j}D_n$$

$$0 = \sum_{j=1}^{N} {}^{ij}A_{ns}{}^{j}D_s + \sum_{j=1}^{N} {}^{ij}A_{nn}{}^{j}D_n \tag{20}$$

At load step (k), an element that has slipped in a previous step can stick in which case the old shear stress S_{old} is 'locked' into the model which is given by

$$S_{old} - K_s\left({}^{i}D_s\right)_{old} = -K_s{}^{i}D_s + \sum_{j=1}^{N} {}^{ij}A_{ss}{}^{j}D_s + \sum_{j=1}^{N} {}^{ij}A_{sn}{}^{j}D_n \tag{21}$$

Eqs. (18)–(21) need to be solved iteratively until all boundary conditions are satisfied.

2.4. Iterative solution techniques

The iterative solution technique, presented in this paper, extends the work of Ameen and Raghuprasad [8] to include closed crack problems. The following algorithm can then be used to solve the problem.

1. Compute the matrices $\boldsymbol{C}$,$\boldsymbol{G}$,$\boldsymbol{E}_1$ and $\boldsymbol{E}_2$ from Eqs. (4), (5), (13) and (14).
2. Factorize matrix $\boldsymbol{C}$ using $[\boldsymbol{C}] = [\boldsymbol{L}][\boldsymbol{U}]$, where $\boldsymbol{L}$ and $\boldsymbol{U}$ are the lower and upper matrices.
3. Calculate $\boldsymbol{D}$ for sub-problem 1.
4. Find the stresses $\boldsymbol{f}_1$ at the internal points corresponding to the crack position of sub-problem 2.
5. The calculated stresses $\boldsymbol{f}_1$ are assumed to act as tractions on the crack faces of sub-problem 2. The crack is assumed closed at all points and the crack face reactions are calculated.
6. Use Eqs. (18)–(21) to calculate the crack discontinuities and tractions.
7. Repeat Steps 8–12 below till sufficient accuracy is obtained
8. Calculate the unknown stresses/displacements $\boldsymbol{f}_2$ from sub-problem 2 at the boundary points of sub-problem 1.
9. Modify the prescribed boundary conditions in sub-problem 1 by subtracting $\boldsymbol{f}_2$ and the new displacement discontinuities are calculated from $\{\boldsymbol{b}\} - \{\boldsymbol{f}_2\} = [\boldsymbol{L}][\boldsymbol{U}]\{\boldsymbol{D}\}$
10. Recalculate the stresses $\boldsymbol{f}_1$ at the internal points corresponding to the crack position of sub-problem 2.
11. The calculated stresses $\boldsymbol{f}_1$ are assumed to act as negative tractions on the crack faces of sub-problem 2.
12. Solve sub-problem 2 using Eqs. (18)–(21).
13. The final displacement and stresses solutions at any point in the body is derived by superposition of the solutions for sub-problems 1 and 2.

It must be noted that LU decomposition is used to factorize matrix $\boldsymbol{C}$ since, in general, step 8 has to be calculated at least four times for open cracks and 10 times for closed cracks before

convergence is achieved. Since LU decomposition only requires back-substitution at each step, this is considerably faster than the full reduction of $\boldsymbol{C}$ at each step.

3. Example problems

The method described in this paper is used to solve two classical fracture mechanics problems. The first problems deals with a central crack in a finite width strip. This open crack problem uses the QDD method to model the exterior plate and the DDT to model the internal crack. The second example problem analyzes a subsurface crack in a half-plane subjected to a moving point load. The second problem has been extensively studied [14–16] because of the interest in rolling contact fatigue failure.

3.1. Example problem 1: open crack problem

Consider a finite width strip with a centrally located crack subjected to a remote tensile stress as shown in Fig. 6. Since the analyzed crack is straight and horizontal, Eqs. (11) and (12) can be further simplified by setting $y = 0$ for G_{ijk} in Appendix A. The normal ($N(x)$) and shear ($S(x)$) tractions are then given by:

$$N(x) = 2\frac{\mu}{\pi(\kappa+1)}\int_{-a}^{a}\frac{B_y(\xi)}{x-\xi}\,\mathrm{d}\xi$$

$$S(x) = 2\frac{\mu}{\pi(\kappa+1)}\int_{-a}^{a}\frac{B_x(\xi)}{x-\xi}\,\mathrm{d}\xi \tag{22}$$

When Eqs. (22) are normalized over the interval $[-1, +1]$ and $s = \xi/a$, it can be shown [12] that the function $B_k(\xi)$ can be rewritten as

$$B_k(s) = \frac{\phi_k(s)}{\sqrt{1-s^2}} \tag{23}$$

Gauss–Chebyshev quadrature gives:

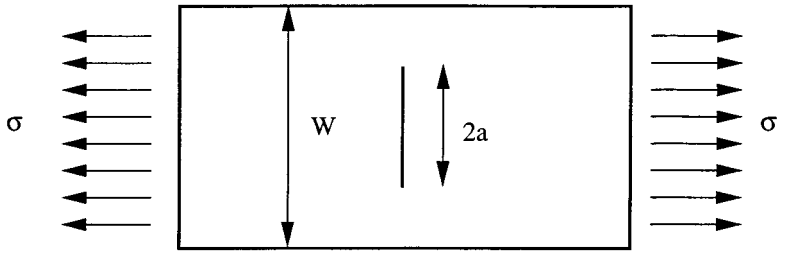

Fig. 6. A cracked tension strip with crack length ($2a$) and width (W).

$$N(t_k) = 2\frac{\mu}{\pi(\kappa+1)}\frac{1}{N}\sum_{i=1}^{N}\frac{\phi_y(s_i)}{t_k - s_i} \tag{24}$$

$$S(t_k) = 2\frac{\mu}{\pi(\kappa+1)}\frac{1}{N}\sum_{i=1}^{N}\frac{\phi_x(s_i)}{t_k - s_i} \tag{25}$$

where N is the number of integration points, $s_i = \cos(\pi\frac{2i-1}{2N})$ are the integration points $(i = 1,\ldots,N)$, $t_k = \cos(\pi k/N)$ are the collocation points $(k = 1,\ldots,N-1)$. In order to solve the system of Eqs. (22) and (23) for the unknowns $\phi_x(s_i)$ and $\phi_y(s_i)$, two further equations are needed.

$$\int_{-a}^{a} B_x(\xi)\,\mathrm{d}\xi = \frac{\pi}{N}\sum_{i=1}^{N}\phi_x(s_i) = 0 \tag{26}$$

$$\int_{-a}^{a} B_y(\xi)\,\mathrm{d}\xi = \frac{\pi}{N}\sum_{i=1}^{N}\phi_y(s_i) = 0 \tag{27}$$

Eqs. (26) and (27) are known as the side conditions, and are obtained from the requirement that the crack faces meet at both ends.

After Eqs. (24)–(27) are solved, the SIF at the crack ends can be calculated using (see Ref. [12])

$$K_{\mathrm{I}}(\pm a) = \pm 2\sqrt{\pi a}\frac{\mu}{\kappa+1}\phi_y(\pm a) \quad \text{and} \quad K_{\mathrm{II}}(\pm a) = \pm 2\sqrt{\pi a}\frac{\mu}{\kappa+1}\phi_x(\pm a) \tag{28}$$

Since $\phi(\pm a)$ are not explicitly calculated in the solution of Eqs. (22)–(25), an extrapolation method must be used. Krenk's extrapolation formulae [12] is a particularly powerful method for finding $\phi(\pm a)$.

Example problem 1 is solved for various crack lengths (a in Fig. 6). The results for the SIF are compared with $K_{\mathrm{I}} = [\sec(\pi a/W)]^{-1/2}\sigma\sqrt{\pi a}$ given by Feddersen [17] and $K_{\mathrm{I}} = [1 -$

Table 1
Comparison of SIF results

	$K_{\mathrm{I}}/(\sigma\sqrt{\pi a})$		
a/W	Dixon	Feddersen	Iterative
0.1	1.0206	1.0254	1.0139
0.2	1.0911	1.1118	1.0942
0.25	1.1547	1.1892	1.1689
0.3	1.2500	1.3043	1.2859
0.4	1.6667	1.7989	1.8190

$(2a/W^2)]^{-1/2}\sigma\sqrt{\pi a}$ given by Dixon [17] in Table 1. The boundary of the strip are discretized using 40 QDD elements and 30 dislocation density integration points are placed on the crack.

Table 1 shows that the iterative technique is within 3% of the analytical solutions. The solution time for the problem on an INDY silicon graphics workstation was 2.23 s for the iterative method. In order to assess the speed of this technique, the same problem was solved using a direct QDD method to model both the boundaries and crack. In order to obtain the same 3% accuracy as the hybrid technique, the QDD method took 1.89 s. When the problem was resolved using double the elements for both methods, the iterative technique required 11.2 s while the QDD method required 14.2 s. Thus, for larger problems, the iterative method is more efficient than the traditional QDD method for solving open crack problems. The iterative technique is faster than the direct approach, since it requires the reduction of a smaller matrix (associated with the uncracked body only) than the direct approach (associated with the full cracked body problem).

3.2. Example problem 2: partially closed crack problem

The growth of a crack parallel to a surface, undergoing periodic compressive loading, is one of the major causes of fatigue damage of riding surfaces. This damage mode has been extensively studied by several authors including the analytical solution of Hearle and Johnson [14], the DDT technique of Chang et al. [15] and the FEM approach of Komvopolous [16]. In order to verify the iterative BEM presented in this paper, the developed iterative technique is compared with the example problem studied by Komvopolous [16].

Consider a horizontal subsurface crack of length $2a$ and depth h subjected to a moving point load (P), as shown in Fig. 7. Depending on the load position (x_p) and crack geometry, various parts of the crack can either undergo forward slip, backward slip, separation or stick as shown in Fig. 8. For this example, the crack-to-depth ratio $2a/h$ is equal to 3, the Young's modulus E is 1×10^{11} N m^{-2} and Poisson's ratio ν is 0.3. The top surface of the elastic half-plane is modeled using 100 QDD elements and the crack is modeled using 25 QDD elements. The shear and normal spring stiffnesses (K_s and $K_n$in Eq. (17) are assumed to be 2×10^{17} N m^{-1}. The coefficient of friction (f) is set equal to 0 and 0.5.

The results of the mode II SIF at the left crack tip and the various modes of crack-opening, closure and stick are compared with the results of Komvopolous [16]. The mode II SIF is calculated from [18]

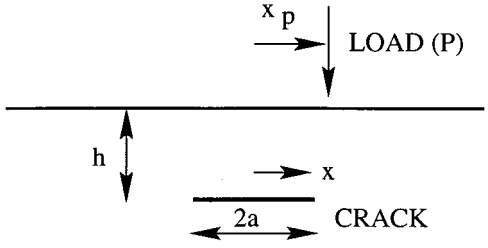

Fig. 7. A subsurface crack in an elastic half-space subjected to a moving point load.

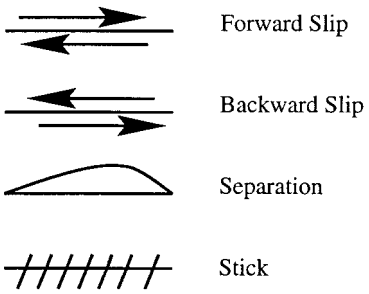

Fig. 8. The stick, slip and separation modes for a closed crack.

$$K_{\mathrm{II}} = \frac{\mu}{4(1-\nu)}\sqrt{\frac{2\pi}{r}}D_{\mathrm{s}}^{\mathrm{tip}}$$

where $D_{\mathrm{s}}^{\mathrm{tip}}$ is the near crack-tip shear discontinuity and r is the distance from the crack tip.

The normalized mode II SIF $K_{\mathrm{II}}/(2P/\pi\sqrt{l})$, for the left crack tip of a frictionless horizontal crack, is compared with the analytical solution of Hearle and Johnson [14] in Fig. 9. The developed iterative BEM shows good agreement with the analytical solution. The crack opening and sliding mechanisms for various normalized load positions (x_p/a) are shown in Fig. 10. The sliding and opening behavior of the crack compare well with the FEM solution of Komvopolous [16]. The mode II SIF for frictionless and frictional contact ($f = 0.5$) for the left

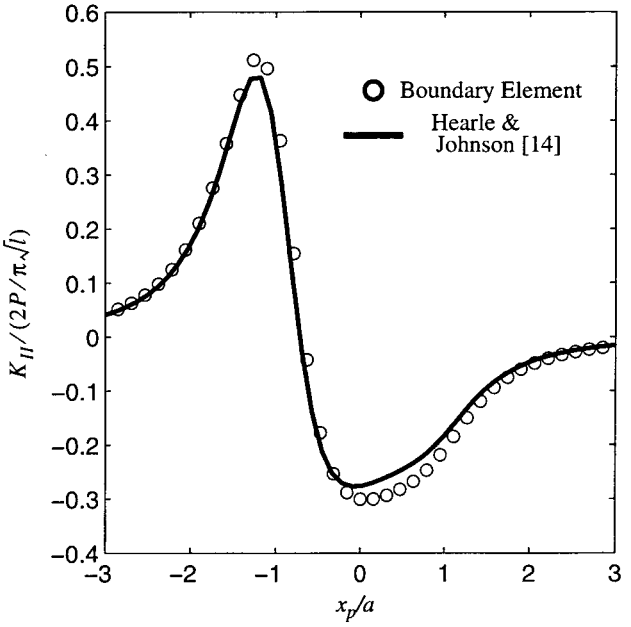

Fig. 9. Comparison of the analytical and boundary element methods for the left crack-tip mode II SIF for a frictionless subsurface crack under various concentrated point load positions.

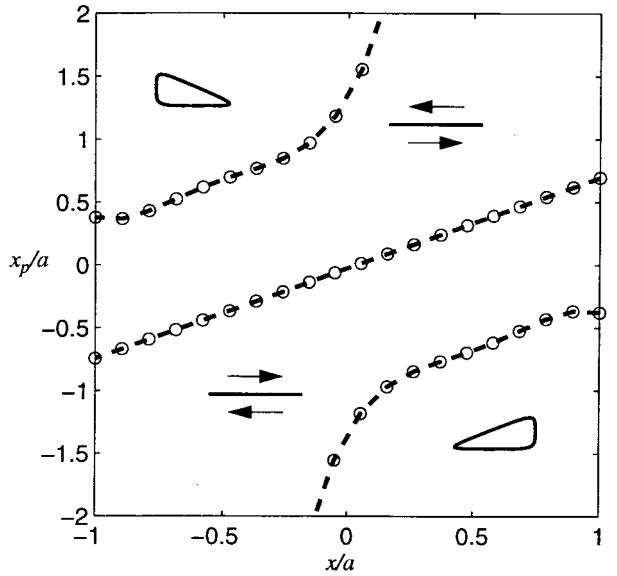

Fig. 10. Regions of slip and separation for the frictionless subsurface crack under various positions of a concentrated point load.

crack tip is shown in Fig. 11. Fig. 11 shows that the consequence of frictional contact is to

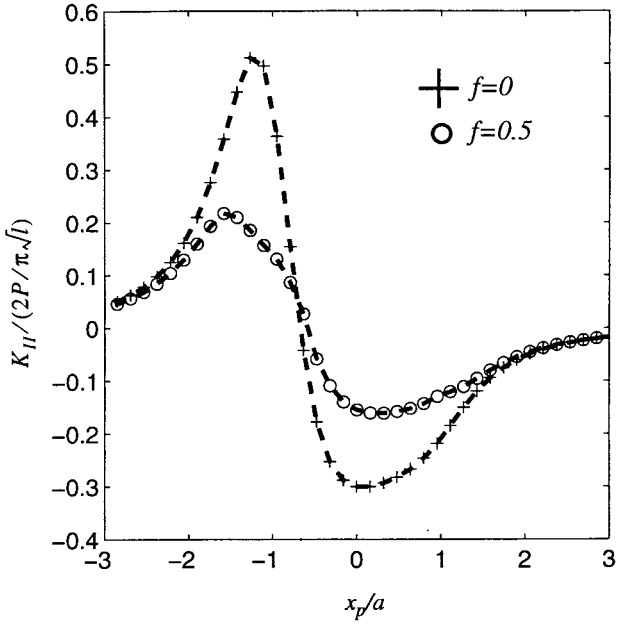

Fig. 11. Comparison of the mode II SIF for the left crack-tip of a frictionless and frictional subsurface crack under various concentrated point load positions.

reduce the SIF for all load positions. Fig. 12 show the various stick, slip and separation zones for various load positions. The results for the frictional contact case compare well with the FEM solution of Komvopolous [16].

Komvopolous' FEM results at $x/a = -1$ and $x/a = 1$; however, show a stick zone near $x_p/a = 2$ and $x_p/a = 2$ which do not appear in Fig. 12. The present analysis is considered correct, since the extent of stick zone at these points can be attributed to the assumed contact convergence parameters used by Komvopoulos [16]. Using a similar FEM model, Komvopoulos and Cho [19] also shows stick at the same locations for deep cracks ($2a/h = 1$). These stick-zones are not consistent with Hearle and Johnson's analysis [14] which show a slip zone, since the driving shear force is greater than the frictional resisting force at a deep crack.

In order to illustrate the solution speed of the new iterative approach, the full problem was solved for all loading positions using the same number of QDD elements (100 on the elastic half-plane and 25 on the crack) and the solution time was compared with the iterative procedure. The solution time for the full problem on an INDY silicon graphics workstation was 2 h, while for the iterative solution was 13 min. The vastly improved speed can be attributed to the fact that the exterior problem's geometry remains the same throughout the solution and can be LU decomposed after the first iteration. Subsequent solutions only requires back-substitution for the exterior problem and the full solution of the much smaller interior crack-problem.

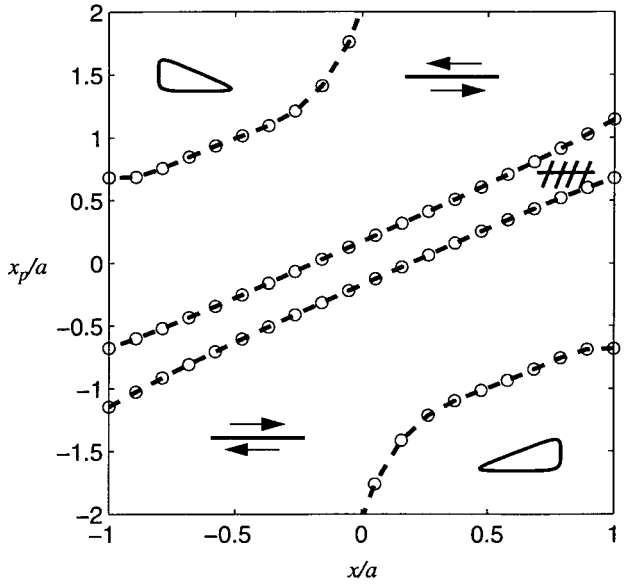

Fig. 12. Regions of slip, stick and separation for the frictional subsurface crack under various positions of a concentrated point load.

4. A note on solution speed

A clear picture of the presented method's solution speed can be garnered by analyzing the two example problems for an increasing number of boundary elements. As previously mentioned, the solution speed of the fast iterative method is compared with the solution speed of the direct QDD method in order to obtain 3% accuracy of the iterative method with the direct solution method. Fig. 13(a) shows the time taken to solve Example problem 1 by both the direct and iterative methods with an increasing number of elements (the number of nodes on both the crack and external boundaries are proportionally increased). Fig. 13(a) shows that the solution time for the open crack case (Example problem 1) increases with increasing number of boundary nodes for both the iterative and direct BEM. As previously discussed, the iterative solution scheme is slower for smaller problems (less than approximately 300 nodes), but is faster for larger problems.

The solution time for solving the closed crack problem (Example problem 2) with an increasing number of boundary nodes is shown in Fig. 13(b). For all problem sizes studied in this case, the iterative BEM was significantly faster (approximately by an order of magnitude) than the traditional direct BEM.

5. Discussions and conclusions

The iterative BEM has been presented in this paper, and has been applied to the modeling of

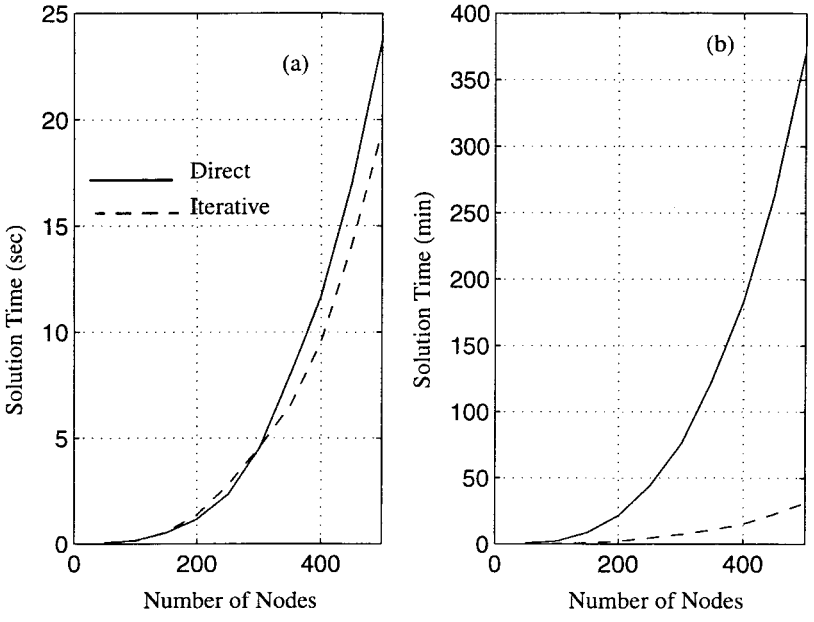

Fig. 13. A comparison of solution speed between the direct and iterative boundary element method with an increasing number of boundary nodes for: (a) Example problem 1; (b) Example problem 2.

closed and open cracks. The method of partitioning the problem into two sub-problems consisting of the exterior body without crack and a crack in an infinite domain has been shown to have some significant advantages over other solution methods. These advantages include:

1. Increased solution speed over large linear elastic (open crack) problems.
2. Vastly increased speed for closed crack problems which involve load-stepping and iteration.
3. The two sub-problems are independently formulated and can be solved with different methods leading to a hybrid approach.
4. The computer matrix-storage space is reduced.

Though this paper has concentrated on dealing with a single isotropic homogenous elastic material, the method can be extended to take into account multi-material anisotropic behavior. Future work could concentrate on analyzing the efficiency of this iterative technique in solving various assumed crack-face mechanisms (such as cracks with cohesion), material constitutive behavior as well as multiple crack problems.

Appendix A

The stress and displacement influence coefficients in Eqs. (6)–(10) are given by

$$G_{xxx} = \frac{-\bar{y}}{r^4}\left(3\bar{x}^2 + \bar{y}^2\right) \tag{A1}$$

$$G_{yxx} = \frac{\bar{x}}{r^4}\left(\bar{x}^2 - \bar{y}^2\right) \tag{A2}$$

$$G_{xyy} = \frac{\bar{y}}{r^4}\left(\bar{x}^2 - \bar{y}^2\right) \tag{A3}$$

$$G_{yyy} = \frac{\bar{x}}{r^4}\left(\bar{x}^2 + 3\bar{y}^2\right) \tag{A4}$$

$$G_{xxy} = \frac{\bar{x}}{r^4}\left(\bar{x}^2 - \bar{y}^2\right) \tag{A5}$$

$$G_{yxy} = \frac{\bar{y}}{r^4}\left(\bar{x}^2 - \bar{y}^2\right) \tag{A6}$$

$$U_{xx} = (\kappa + 1)\Theta + \frac{2\bar{x}\bar{y}}{r^2} \tag{A7}$$

$$U_{xy} = -(\kappa - 1)\log r - \frac{2\bar{x}^2}{r^2} \tag{A8}$$

$$U_{yx} = -(1-\kappa)\log r - \frac{2\bar{x}^2}{r^2} \tag{A9}$$

$$U_{yy} = (\kappa+1)\Theta - \frac{2\bar{x}\bar{y}}{r^2} \tag{A10}$$

where $\bar{x} = x - x_d$, $\bar{y} = y - y_d$, $r^2 = (x-x_d)^2 + (y-y_d)^2$ and Θ is the angle shown in Fig. 3.

References

[1] Lee SS. Complementarity problem formulation for the crack closure problem using the dual boundary element. In: Proceedings of the 1997 Third International Conference on Contact Mechanics. 1997. p. 289–99.
[2] Sirtori S, Maier G, Novati G, Miccoli S. A Galerkin symmetric boundary element method in elasticity: formulation and implementation. International Journal of Numerical Methods in Engineering 1976;10:301–43.
[3] Blanford GE, Ingraffea AR, Liggett JA. Two-dimensional stress intensity factor computations using the boundary element method. International Journal of Numerical Methods in Engineering 1992;35:255–82.
[4] Crouch SL. Solution of plane elasticity problems by the displacement discontinuity method. Part I: Infinite body solution; Part II: Semi-infinite body solution. International Journal of Numerical Methods in Engineering 1976;10:301–43.
[5] Hong HK, Chen JT. Derivation of integral equations in elasticity. Journal of Engineering Mechanics 1988;114:1028–44.
[6] Gray LJ. Boundary element method for regions with thin internal cavities. Engineering Analysis 1989;6:180–91.
[7] Portela A, Aliabadi MH, Rooke DP. A dual boundary element method: effective implementation for crack problems. International Journal of Numerical Methods in Engineering 1992;33:1269–87.
[8] Ameen M, Raghuprasad BK. Hybrid technique of modeling of cracks using displacement discontinuity and direct boundary element method. International Journal of Fracture 1994;67:343–55.
[9] Sturt A, Nowell D, Hills DA. Application of the boundary element and dislocation density methods in plane crack problems. Engineering Analysis with Boundary Elements 1993;11:129–35.
[10] Xu G, Ortiz M. A variational boundary integral method for the analysis of 3D cracks of arbitrary geometry modelled as continuous distributions of dislocation loops. International Journal of Numerical Methods in Engineering 1993;36:3675–701.
[11] Bhattacharyya PK, Willment T. Quadratic approximations in the displacement discontinuity method. Engineering Analysis 1988;5:28–35.
[12] Hills DA, et al. Solution of crack problems: the distributed dislocation technique. Boston: Kluwer Academic Publishers, 1996.
[13] Crouch SL. Computer simulation of mining in faulted ground. Journal of the South African Institute of Mining and Metallurgy 1979;79:159–73.
[14] Hearle AD, Johnson KL. Mode II stress intensity factors for a crack parallel to the surface of an elastic half-space subjected to a moving point load. Journal of the Mechanics and Physics Solids 1985;33:61–81.
[15] Chang FK, Comninou M, Sheppard S, Barber JR. The subsurface crack under conditions of slip and stick caused by a surface normal force. Journal of Applied Mechanics 1984;51:311–6.
[16] Komvopolous K. Subsurface crack mechanisms under indentation loading. Wear 1996;199:9–23.
[17] Ewalds HL, Wanhill RJ. Fracture Mechanics. Australia: Edward Arnold, 1986.
[18] Zhang S, Leech CM. FEM analysis of mixed mode fracture of CSM-GRP. Engineering Fracture Mechanics 1986;23:521–35.
[19] Komvopoulos K, Cho S-S. Finite element analysis of subsurface crack propagation in a half-space due to a moving asperity contact. Wear 1997;209:57–68.